Precipitation-driven typology of storms in the Alps

Georgia Papacharalampous[1,*], Eleonora Dallan[1], Moshe Armon[2], Joydeb Saha[1,3], Colin Price[4], Marco Borga[1], and Francesco Marra[5]

[1] Department of Land, Environment, Agriculture and Forestry, University of Padova, Legnaro, Italy

[2] The Fredy and Nadine Herrmann Institute of Earth Sciences, The Hebrew University of Jerusalem, Jerusalem, Israel

[3] National Centre for Medium Range Weather Forecasting, Noida, India

[4] Porter School of the Environment and Earth Sciences, Tel Aviv University, Tel Aviv, Israel

[5] Department of Geosciences, University of Padova, Padova, Italy

[*] Correspondence: georgia.papacharalampous@unipd.it, papacharalampous.georgia@gmail.com

Precipitation-driven typology of storms in the Alps

Georgia Papacharalampous[1,*], Eleonora Dallan[1], Moshe Armon[2], Joydeb Saha[1,3], Colin Price[4], Marco Borga[1], and Francesco Marra[5]

[1] Department of Land, Environment, Agriculture and Forestry, University of Padova, Legnaro, Italy

[2] The Fredy and Nadine Herrmann Institute of Earth Sciences, The Hebrew University of Jerusalem, Jerusalem, Israel

[3] National Centre for Medium Range Weather Forecasting, Noida, India

[4] Porter School of the Environment and Earth Sciences, Tel Aviv University, Tel Aviv, Israel

[5] Department of Geosciences, University of Padova, Padova, Italy

[*] Correspondence: georgia.papacharalampous@unipd.it, papacharalampous.georgia@gmail.com

Abstract: Advances in precipitation science often depend on categorizing storms into homogeneous classes, particularly convective- and stratiform-like. To address this need, this study introduces an Alpine storm typology derived from the pairing of a vast sub-hourly gauge dataset, comprising over 790,000 independent storms, with an objective method, driven solely by precipitation features and optimized for big data clustering. Five dominant classes were identified from this partition, with distinct clustering fingerprints in maximum intensity, total volume, total duration and temporal variability, alongside clear spatial organization. Additional traits (initiation month, peak solar time, lightning count) and comparisons with radar-based benchmarks suggest that one class is likely associated with convective-like extremes (high intensity, summer/afternoon peaks, high lightning) and another with stratiform-like behaviors (medium intensity, large volume, long duration, low lightning), while the remaining classes gather moderate and minor storms. The typology could support applications such as class-specific stochastic simulation, class-informed bias adjustment of climate projections or multi-class extreme value analyses. Climatological investigations revealed, among others, higher convective-like activity in recent years and specific regions, offering direct evidence on evolving hazard risks. We provide the historical occurrences of the classes as an open dataset to facilitate further investigation of Alpine storm dynamics and their implications.

Keywords: big data clustering; convective-stratiform; hydro-climatological trends; storm climatology; storm features; sub-hourly precipitation

1. Introduction

Analyzing precipitation storms and their climatology is crucial for mitigating hazards such as floods, landslides and debris flows, alongside adapting to changing climatic conditions (D'Odorico et al. 2005; Merz et al. 2014; Breugem et al. 2020; Kahraman et al. 2021). Key to these efforts is separating storms into homogeneous classes, similar to flood and other hydrological event categorizations (e.g., Hirschboeck 1988; Merz and Blöschl 2003; Turkington et al. 2016; Oppel and Fischer 2020), but with the focus here being on the convective-stratiform partition (e.g., Tremblay 2005; Ruiz-Leo et al. 2013; Feloni et al. 2019; Sottile et al. 2022; Dallan et al. 2022; Araujo et al. 2023; Treppiedi et al. 2023; Laaha et al. 2025). Beyond its role in advancing our comprehension of precipitation dynamics through contrasting storm behaviors, this separation has direct implications for stochastic modelling, extreme value analysis and model uncertainty reduction (Blöschl et al. 2019; Fischer et al. 2019; Fischer and Schumann 2021; Marra et al. 2021; Sottile et al. 2022), consistent with the markedly different hydrological hazards associated with the respective types (e.g., localized flash floods versus widespread fluvial flooding). This, in turn, underpins the development of tailored weather generators (e.g., Kaczmarska et al. 2014; Peleg and Morin 2014; Tseng et al. 2025; Laaha et al. 2025) and operational forecasting models (e.g., Papadopoulos et al. 2005; Gustafsson et al. 2018; Zhou et al. 2019), or class-specific bias correction methods for climate model simulations (Maraun et al. 2017).

At the same time, deriving storm typologies that meaningfully reflect such domain knowledge and modelling requirements remains challenging. This difficulty stems from the inherent complexity of the distinct mechanisms driving storm generation within each class, with the underlying physical interactions spanning multiple spatiotemporal scales (Grazzini et al. 2019), as well as the scarcity of measurements of key physical variables at relevant resolutions (e.g., vertical lifting velocities at hundreds of meters). This challenge is even more pronounced, yet often necessary to confront, by relying solely on gauge precipitation data. For this particular setting, which is also the focus of this study, traditional manual thresholds on maximum intensity or decorrelation time (e.g., those by Dallan et al. 2022; Araujo et al. 2023) introduce a strong degree of subjectivity. Ongoing efforts thus target their replacement with more objective means, such as curve- (e.g., Sottile et al. 2022; Treppiedi et al. 2023) and feature-based clustering (e.g., Grazzini et al.

2019; Laaha et al. 2025) from the unsupervised machine learning family (Hastie et al. 2009, ch. 14; James et al. 2013, ch. 10).

A general storm typology for the Alpine range, a geographically complex territory attracting major interest in precipitation dynamics (e.g., Frei and Schär 1998; Weisse and Bois 2001; Isotta et al. 2014; Ménégoz et al. 2020; Napoli et al. 2023; Estermann et al. 2025) and hydrological extremes (e.g., Blanchet et al. 2025) is still lacking. Existing regional classification frameworks are constrained by an exclusive focus on precipitation extremes (e.g., Grazzini et al. 2019), restricted spatial domains (e.g., northern Italy in Grazzini et al. 2019, or a single Austrian location in Laaha et al. 2025) and closed data formats. Furthermore, dependencies on multiple broad atmospheric variables or ex-situ data (e.g., Grazzini et al. 2019; Flaounas et al. 2023; Laaha et al. 2025) could limit the geographic transferability of cluster analyses due to data unavailability or highly localized processing protocols. Such dependencies can also compromise the identification of localized rainfall patterns due to typically coarse grids. For these reasons, prior studies lack extended climatological analyses, which are, among others, essential for detecting long-term trends in storm-class frequencies (e.g., Rulfová and Kyselý 2013; Llasat et al. 2021; Treppiedi et al. 2023). Such analyses may provide direct evidence regarding how the ongoing climate change is altering the balance between contrasting storm types, thereby also shaping the evolution of future hazard risks.

To address these gaps, this study presents the first objective, robust and transferable Alpine precipitation storm typology with no dependency on ex-situ data. This dependency was eliminated by formulating and leveraging a collection of 792,786 high-resolution, sub-hourly precipitation storm time series of varying characteristics (Appendix A). In terms of volume, this collection surpasses the largest existing precipitation storm collections (e.g., Villalobos Herrera et al. 2023), as well as other remarkably large event databases in the field (e.g., Stein et al. 2020; Tarasova et al. 2020). Recorded across five countries in the Alpine territory (Figure S1), it further ensures the intended generalizability across the target, regional hydro-climatic regimes. More precisely, our aims were to: (i) establish a domain-informed separation of contrasting precipitation storm behaviors in the Alps, provided as an open dataset; and (ii) characterize the climatology of the storm classes by detecting trends in their proportions over time, alongside analyzing spatial and seasonal variations, to ultimately reveal evolving current

and future hazard risks across the region.

2. Results and discussion

2.1 Overall storm type profiles and associated water-related hazards

Five Alpine storm classes emerged from the clustering analyses, exhibiting distinct and potentially physically suggestive profiles based on the collective analysis of their driving (Figure 1a–d), additional diagnostic storm-level features (Figure 1e–g) and spatial co-occurrence patterns (Text S1, Figure S3), with the latter two components reflecting key physical aspects that were deliberately omitted from the clustering to maintain simplicity:

- "Type-1 major" (156,295 storms): The highest maximum instantaneous intensities, among the highest total volumes, the highest coefficient of variation values, pronounced summer and afternoon peaks, strong association with lightning activity, and a high degree of spatial clustering with persisting co-occurrence over 500 km. – Associated water-related hazards: High-impact localized flash floods, landslides, debris flows and urban drainage overloads.
- "Type-2 major" (182,309 storms): Medium maximum intensities, the highest total volumes, the longest total durations, low coefficient of variation values, a bimodal seasonal distribution peaking in spring and autumn, an almost flat diurnal cycle, minimal associated lightning activity, and a high degree of spatial clustering with persisting co-occurrence over 500 km. – Associated water-related hazards: High-impact widespread, regional floods.
- "Moderate" (190,385 storms): Maximum intensities and coefficients of variation values of similar magnitude as the "type-2 major" class, somewhat smaller total volumes, much shorter durations, relatively flat seasonal and diurnal distributions, negligible associated lightning activity, and a moderate degree of spatial clustering. – Associated water-related hazards: Minor flooding and surface runoff disruptions.
- "Type-1 minor" (136,056 storms): Mostly low maximum intensities, mostly low total volumes, medium total durations, high coefficient of variation values, storm time series punctuated by relatively long dry periods (from visual inspection), relatively flat seasonal and diurnal distributions, negligible associated lightning activity, and a localized nature indicated by the abrupt reduction in spatial co-occurrence at short distances. – Associated water-related hazards: Negligible/none.

- "Type-2 minor" (127,741 storms): Mostly low maximum intensities, mostly low total volumes, short total durations, low coefficient of variation values, relatively flat seasonal and diurnal distributions, negligible associated lightning activity, and a localized nature indicated by the abrupt reduction in spatial co-occurrence at short distances. – Associated water-related hazards: Negligible/none.

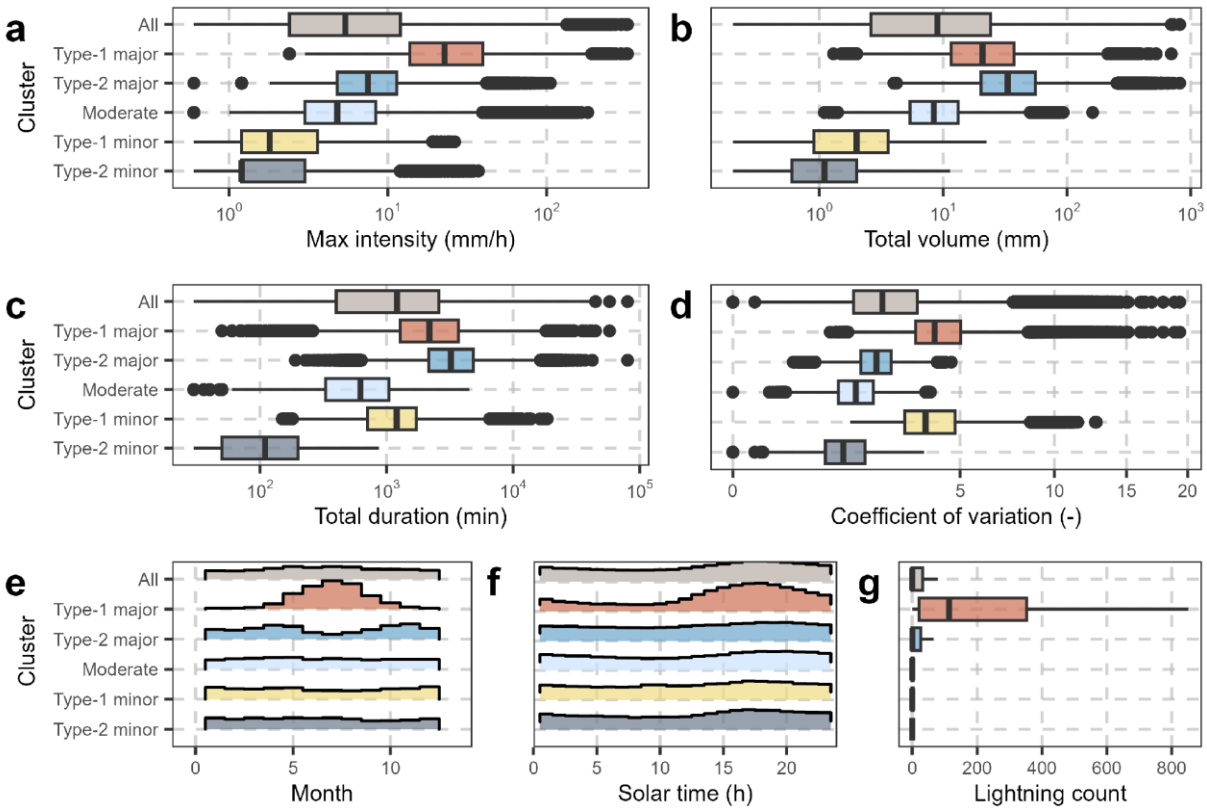

Figure 1. Analysis of the (a–d) driving and (e–g) additional diagnostic storm-level features of the five storm classes. In panel (g), outliers have been removed for visual clarity. The relationships between the driving features can be inspected by class in Figure S2.

Figure 2 provides an intuitive understanding of the spatial dynamics and their seasonal variations, as well as a more complete perspective on the classes, by displaying the geographical distribution of storms across the Alpine range during both random dates and dates with major, high-impact events. In winter and early spring (Figure 2a, c, e), the "type-2 major", "moderate", "type-1 minor" and "type-2 minor" storm classes display noticeable spatial clustering, which is most pronounced in the first two. In contrast, "type-1 major" storms appear randomly distributed. However, during dates with high-impact events (Amponsah et al. 2016; Destro et al. 2018; Borga et al. 2019; Gabella et al. 2019; Davolio et al. 2020) in autumn and summer (Figure 2b, d, f–h), both "major" classes exhibited strong spatial clustering, often extending over large areas, while both "minor"

classes occurred only sporadically, typically on the periphery of the wet region.

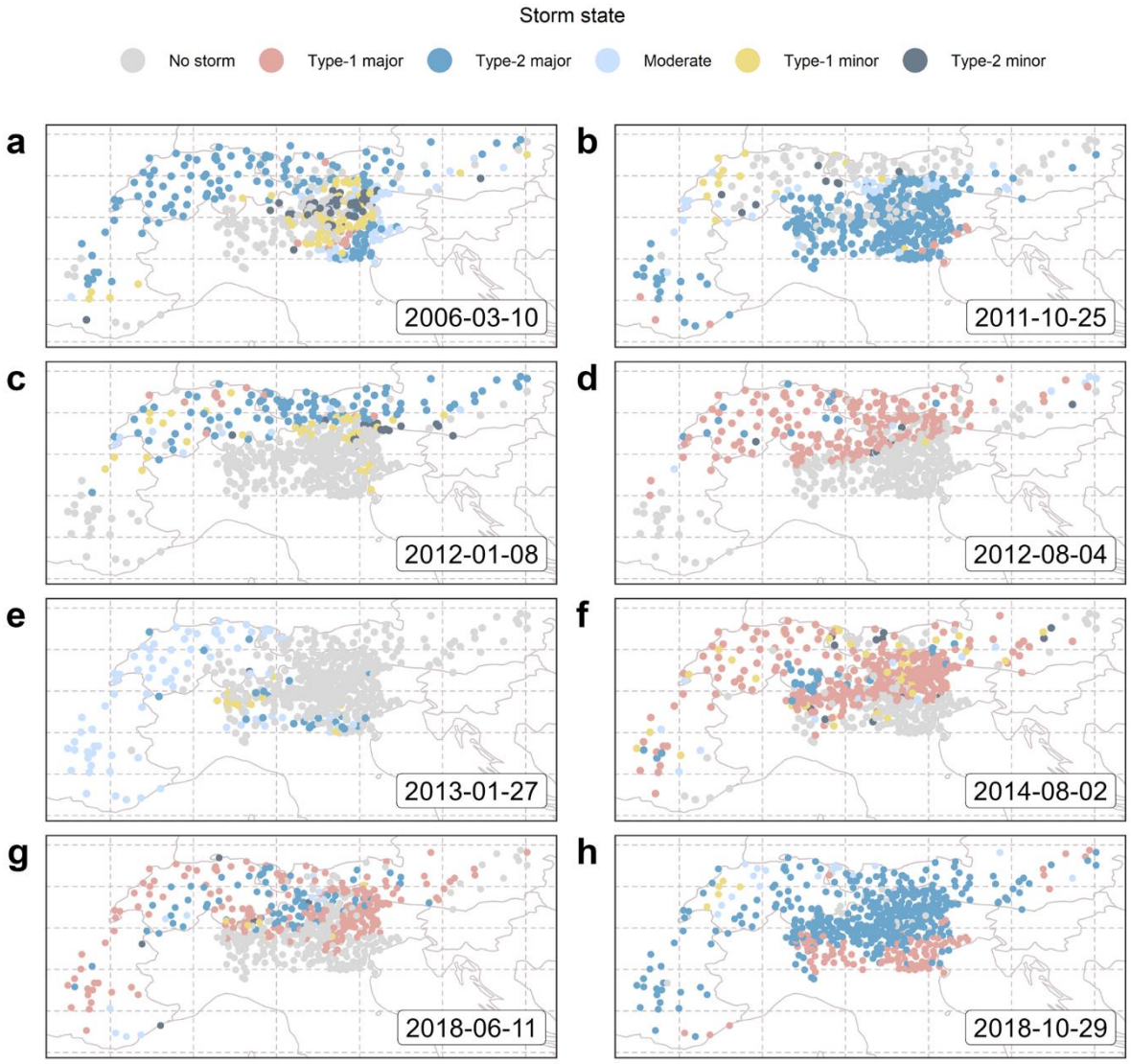

Figure 2. Storm state at stations with data on (a, c, e) random dates in the winter or early spring and (b, d, f–h) dates with well-documented storm events occurred.

2.2 Detailed storm climatological profiles and operational implications

Beyond overall storm type profiling, our dataset reveals distinct spatial patterns in the occurrence rates of the Alpine storm types (Text S2, Figure S4), which directly translate into regional hazard exposures based on the linkages with water-related hazards detailed in Section 2.1. In general, "type-2 major" storms are broadly spatially distributed across the Alpine territory (comprising 20–40% of all storms), underlining the continuous, domain-wide baseline likelihood of large-scale, multi-basin flooding that challenges regional water management and transboundary hazard mitigation. Conversely, the "type-1 major" storms (10–30%) are most frequent in north-eastern Italy, signaling an elevated

likelihood of localized, fast-responding water-related hazards that acutely reduce the required emergency response windows. At the same time, the rates of the minor and moderate classes exhibit less spatial variability, although the "type-1 minor" storms occur more frequently in the north Italian lowlands, consistent with the localized nature of this class, as evidenced by its rapid decay in spatial co-occurrence (Figures 2 and S3).

Regarding seasonal dynamics across the region, the "type-1 major" storm rates, and therefore also the required emergency response times, exhibit a distinct south-to-north and lowland-to-highland gradient during summer (Text S3, Figure S5). On the contrary, the "type-2 major" storms exhibit high occurrence frequencies (40–50%) during spring and autumn across the entire region, without clear spatial patterns, pointing to the necessity of maintaining synchronized, region-wide flood mitigation strategies during these seasons. Meanwhile, the "moderate" storms remain uniformly distributed across all seasons and locations, constituting a steady background driver for routine hydrological regimes and defining their regular operational baseline.

Complementing these spatial and seasonal climatologies, our trend analysis reveals a distinct, long-term shift in the balance of the Alpine storm regimes, marked by an intensification of "type-1 major" behaviors, alongside a decline in "type-2 major" and "moderate" events (Figure 3). While upward trends for the "type-1 major" storms span all seasons (Figure 3a, d), they are far more prevalent in summer (Figure 3b, c, e, f), reaching statistical significance at about 27% of the long-record stations (Figure 3e). Concurrently, the negative temporal changes for the "type-2 major" and "moderate" classes are also more pronounced in summer (Figure 3b, e), with statistically significant trends for roughly 16% and 19.5% of the long-record stations, respectively. This simultaneous coupling of rising "type-1 major" frequencies and decaying volumetric events implies a transition toward flashier, more erratic water-related hazards, requiring civil protection frameworks to emphasize responsive, impact-based early warning systems.

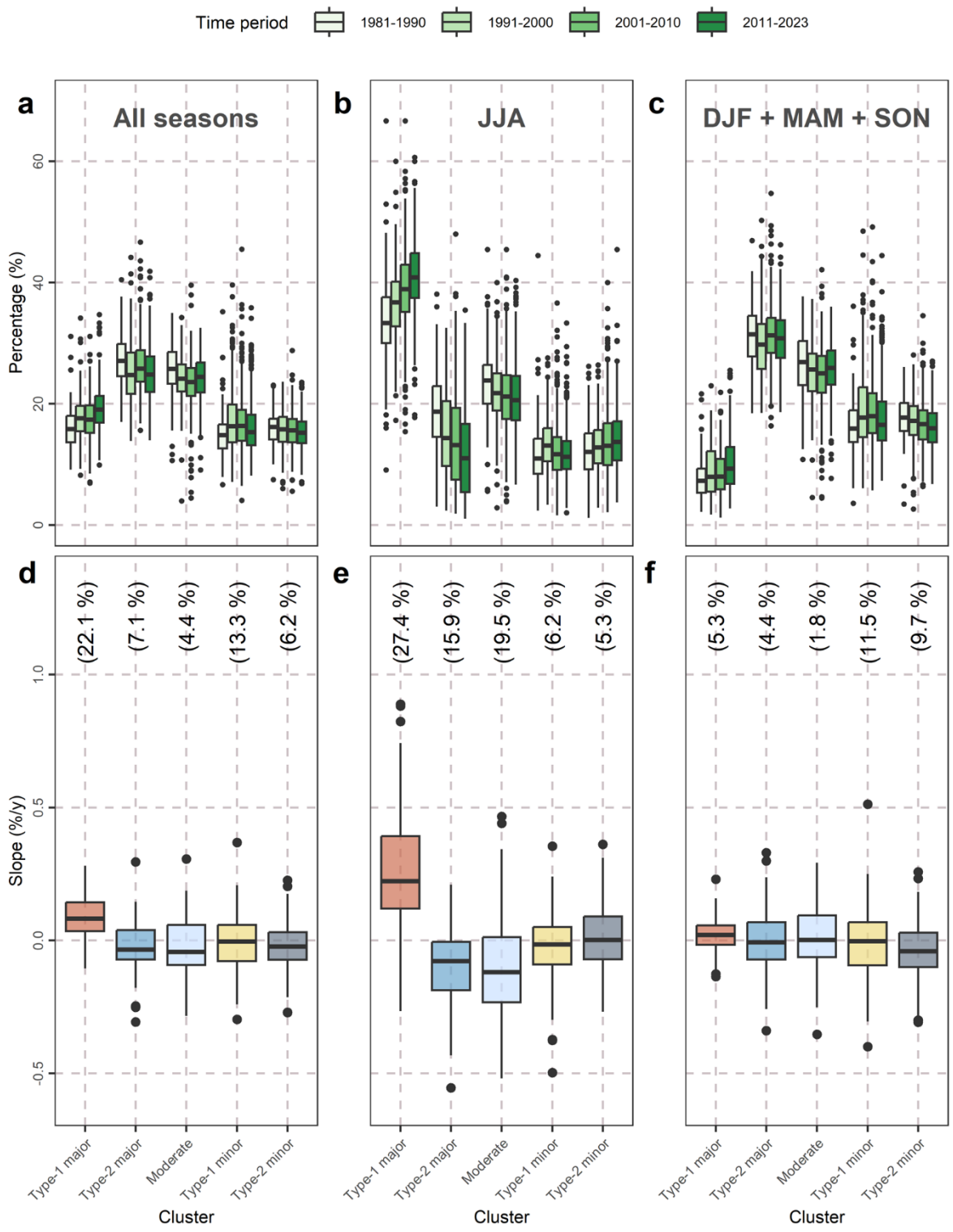

Figure 3. Analyses of the temporal changes in the occurrence rates of the classes at the various stations: (a-c) Percentages of the classes within consecutive time periods, and (d-f) trend analyses for the 113 stations with at least 30 complete years of precipitation data (see Figure S1), with the percentages of the stations with statistically significant trends reported at the top of the side-by-side boxplots of the linear slope estimates.

2.3 Plausible process attribution and typology robustness

The derived profiles of the "type-1 major", "type-2 major" and "moderate" storm classes (Sections 2.1 and 2.2) point to their plausible associations with distinct precipitation processes. Specifically, the "type-1 major" regime is convective-like, a plausible link that emerges by pairing its baseline traits (Section 2.1) with both the warm-season lowland-to-highland gradient (Figure S5), reflecting the well-investigated orographic uplift over the pre-Alpine and Alpine terrain, and the notable temporal increase in its occurrence (Figure 3). Indeed, Dallan et al. (2022) reported increasing trends in extreme short-duration precipitation in the north-eastern Italian Alps and attributed them to enhanced convective activity in summer. Our results may suggest that this signal extends beyond the area analyzed by these authors to the entire Alpine region, though further investigation would be needed to confirm this interpretation. Recent findings by Dallan et al. (2024), Estermann et al. (2025) and Peleg et al. (2025) indicate that this increasing trend in heavy precipitation is expected to continue in the future, based on analyses of climate model projections.

When considering such potential linkages, it is essential to account for the station-based (or time series-based) nature of our storm typology. For instance, the long total duration of the "type-1 major" class, which might initially appear inconsistent with typical convective event features, is clarified by our methodological context (Section 4): our method classified the entire storm time series (separated from adjacent storms by at least one dry day, and possibly comprising periods with diverse characteristics, including relatively long dry spells), rather than isolating its “convective” component. Similarly, the extensive spatial clustering observed for the same class, while seemingly at odds with intuitions about localized convection, becomes understandable when considering that individual convective cells are advected and can cover relatively large areas over the storm lifetime, and that the conditions favourable of generating convection may prevail over larger areas compared with the cell size, so there is a high chance of convection occurring at some point during the day over the area experiencing these conditions.

Meanwhile, the "type-2 major" storms exhibit features typical of stratiform events (Section 2.1). Notably, the physical interpretation of both major, high-impact storm types is supported by Marra et al. (2026), who, using our classification, demonstrated that most sub-hourly extremes are “type-1 major” rather than “type-2 major” storms, while around

70% of the 24-hour extremes are “type-2 major” storms (compared to 30% for “type-1 major”). The same physical interpretation is further supported by historical benchmarks extensively documented through radar datasets:

a) October 25, 2011 (Figure 2b): Heavy rainstorms with large spatial extent in northern Italy, characterized as “stratiform” in Amponsah et al. (2016), are attributed to the “type-2 major” class.

b) August 4, 2012 (Figure 2d): The storm that led to a severe flash flood and numerous debris flows in the Vizze valley in the eastern Italian Alps, identified as a highly “convective” event by Marra et al. (2014) and Destro et al. (2018), is attributed to the “type-1 major” class.

c) August 2, 2014 (Figure 2f): Characterized as a “convective” event by Borga et al. (2019), this short-duration intense storm that caused the Lierza river in the eastern Italian Prealps to burst its banks, leading to severe flash flooding and landslides in Veneto, northern Italy, is attributed to the “type-1 major” class.

d) June 11, 2018 (Figure 2g): The heavy thunderstorms and a record-breaking, high-intensity, short-duration storm that caused flash flooding in Lausanne, Switzerland, characterized as highly “convective” by Gabella et al. (2019), are attributed to the "type-1 major” class.

e) Late October, 2018 (Figure 2h): Characterized as a broad “stratiform” system with embedded “convective” cores by Davolio et al. (2020), the Vaia storm that severely hit north-eastern Italy is attributed to “type-2 major” class, with vast regions of “type-1 major” features, mostly in the southern lowlands.

For the "moderate" class, we hypothesize an association with stratiform events where winds run orthogonal to the main cloud direction, yielding traits similar to typical stratiform systems but with shorter total durations (Section 2.1). On the other hand, no process attribution can be confidently attempted for the minor types. Given the station-based nature of our storm typology, these likely reflect intermittent gauge exposure to the periphery or weaker margins of larger-scale storms rather than separate precipitation storm regimes, underscoring the inherent challenges of establishing a fully definitive, physically consistent typology solely from point measurements. Of course, it is important to emphasize that the interpretations offered here, although plausible, are not physically definitive, as our classification remains statistically based and data-driven. Establishing such physical linkages definitively would require different types of investigations, beyond

the aims and contributions of this study and based on information that is not necessarily available at the scales of interest.

Overall, the five-class typology proposed herein captures the Alpine precipitation dynamics well by isolating the anticipated high-intensity/high-volume ("type-1 major") and long-duration/high-volume ("type-2 major") regimes, alongside “moderate” and low-intensity "minor" storm instances. Alternative setups were tested during the study, but introduced redundancy or failed to isolate homogeneous regimes. For instance, a six-cluster configuration merely split a primary class into two subgroups lacking clear domain differentiation. Notably, the five classes are highly robust to data subsampling (including the removal of entire regions), yielding stable feature profiles. This stability satisfies a critical event typology criterion (Tarasova et al. 2019) that is often difficult to achieve with standard clustering methods (James et al. 2013, ch. 10.3.3). Furthermore, this five-class configuration closely aligns with previous storm classifications, in particular the "mixed" or "unresolved" classes by Rulfová and Kyselý (2013) and Cipolla et al. (2020), the convective-stratiform dynamics identified by Sottile et al. (2022), and the heavy storm classes of “frontal”, “intermediate” and “deep convective” by Grazzini et al. (2020).

3. Conclusion

This study introduces an Alpine precipitation storm typology that comprises two clearly distinguished high-impact classes, one convective-like (characterized by high sub-hourly maximum intensity, summer/afternoon peaks and accompanying high lightning activity) and one stratiform-like (characterized by medium sub-hourly maximum intensity, large volume, long duration and minimal lightning activity). Given this consistency with domain knowledge, which is demonstrated through extensive investigations into storm-level features, spatial co-occurrence patterns and radar-based benchmarks of historical high-impact events across the region, the complete labeled database is provided as an open dataset (Appendix A) to support future applications in stochastic simulation, climate modelling and extreme value analysis. Such class-informed modelling is needed, as contrasting storm behaviors translate directly into contrasting water-related hazard profiles, with convective-like storms triggering localized flash floods, landslides and debris flows, and stratiform-like storms causing widespread fluvial flooding and other regional-scale disasters.

Climatological analyses revealed an upward trend in the occurrence frequencies of convective-like storms, signaling an escalating risk of localized water-related hazards, particularly during summer. They also demonstrated that these frequencies vary with both location and season, identifying regions where they are higher than in others for specific seasons, such as the lower-elevation regions in Italy during spring, pointing to an earlier-starting and more prolonged seasonal window for convective-related hazards in these areas. These findings underscore the potential of the proposed typology for revealing new aspects of the Alpine precipitation dynamics and their implications in relation to hydrological engineering design and real-time hazard mitigation. This potential is additionally reflected in the straightforward integration of the typology into frameworks for extreme precipitation characterization and modelling, as well as the resulting insights (Dallan et al. 2025; Marra et al. 2026). While direct validation against large-scale weather types remains non-trivial due to the scale mismatch between synoptic atmospheric states and point precipitation gauges, exploring this connection even in a simplified form represents a key path forward to enhance the physically-grounded applicability of the proposed typology.

4. Methods

4.1 Study area and data

We studied storms that have occurred in and around the Alps (Figure S1), a region with a wide range of climates, mainly alpine (polar), boreal (snow) and warm temperate, according to both the present-day and future Köppen-Geiger classifications by Beck et al. (2023). Largely due to the strong influence of mountainous topography on local precipitation especially near the sea (Buzzi et al. 1998), the Alps offer a compelling setting for the study of precipitation storm patterns and their climatology (Rubel et al. 2017). Compared to other regions, the Alps exhibit a higher proportion of high-intensity wet days (Isotta et al. 2014), a larger proneness to extreme storms (Grazzini et al. 2019) and higher lightning counts (Kahraman et al. 2022). The precipitation climatology of the greater Alpine region has been analyzed, for instance, by Frei and Schär (1998), Isotta et al. (2014), Ménégoz et al. (2020) and Napoli et al. (2023). The mean annual precipitation is typically higher than the surrounding floodplains due to orographic enhancement, reaching values as high as 3000 mm $year^{-1}$. The central region receives lower precipitation amounts, on the order of 900 mm $year^{-1}$, due to the protection effect played

by the surrounding mountains (Borga et al. 2005).

To capture these precipitation dynamics, we compiled a comprehensive dataset of sub-hourly precipitation measurements from seven data sources (Appendix A) and 670 instrumental stations across five countries (Figure S1): Italy (505 stations), Austria (74 stations), Switzerland (61 stations), France (27 stations), and Germany (3 stations). Based on the Amazon Web Services Terrain Tiles (https://registry.opendata.aws/terrain-tiles), the elevations at the locations of the stations range between –4 and 3,214 m, with a mean and a standard deviation approximately equal to 773 and 627 m, respectively. Our dataset was formulated by building upon, modifying and expanding previous data compilation efforts for the region. Specifically, subsets of this dataset were previously compiled and utilized in the studies by Dallan et al. (2023, 2024), Marra et al. (2024), Correa-Sánchez et al. (2025) and Peleg et al. (2025).

From the original sources, time series of varying temporal resolutions (5-, 6- and 10-min) were extracted and homogenized through time series aggregation to the 10- or 12-min temporal resolution (the latter specifically for the network in France). Additionally, time zone homogenization was conducted and quality issues (i.e., missing values/dates, negative and other unrealistic values, duplicate dates) were identified and treated. Time series data records corresponding to calendar years with more than 10% of their values missing were excluded from our final dataset. This dataset comprises complete sub-hourly precipitation time series with varying lengths, observed during the course of 44 years (1981–2024). From these time series, we subsequently extracted the precipitation storm time series, as detailed in Section 4.2. The number of complete calendar years per location is summarized in Figure S1. Data for at least 30 complete calendar years are available for 113 locations, allowing for trend analyses (Section 4.6).

In addition to these rainfall measurements, lightning count data were integrated into our database. As there is a well-known association between convective precipitation and lightning occurrence (Soriano et al. 2001; Papadopoulos et al. 2005; Pineda et al. 2007), lightning counts can be used to investigate distinctions between convective-like and other storm time series (Feloni et al. 2019). Such data, and more precisely cloud-to-ground lightning counts derived from the World Wide Lightning Location Network (WWLLN; https://wwlln.net), are available for a large and representative portion of the stations and storms we examined. Herein, we exploited them in our post-clustering investigations (Section 4.4). Detailed information about the WWLLN network can be found in Rodger et

al. (2006) and Virts et al. (2013). Given that the storms often spanned multiple days, the maximum daily lightning count was extracted for each storm. To ensure consistency and account for uncertainty in the geolocation, lightning strikes were counted within a ±0.5° grid box centered on the location of each station. Temporal alignment was achieved by matching the WWLLN lightning data to the storm time ranges.

4.2 Storm time series extraction

Precipitation storm time series, representing wet periods that are independent in time, were extracted from the precipitation dataset (Section 4.1) following the methodology described in Marra et al. (2020). Considering the climatology of the Alps, independence was ensured by imposing the lower threshold of 24 hours in the length of the dry spells between storms. Storms with a duration of at least 30 min were included in our precipitation storm database.

4.3 Storm clustering

To classify the precipitation storm time series, we formulated a methodology employing unsupervised machine learning. This approach is increasingly used for developing storm typologies (e.g., Grazzini et al. 2019; Sottile et al. 2022; Laaha et al. 2025) and, more generally, event typologies in the field of hydrology (e.g., Markonis et al. 2021; Fischer and Schumann 2024), owing to its objectivity and scalability, qualities that align well with the objectives of this study. Our clustering methodology is feature-based, aiming at maximizing intra-cluster homogeneity and inter-cluster heterogeneity based on the following four diverse features extracted from the precipitation storm time series (Section 4.2): (a) maximum (peak) intensity, (b) total volume, (c) total duration, and (d) coefficient of variation. The diversity and pairwise relationships of these selected features can be inspected in Figure S2. The first three of them, in particular, are established as key features in the study of storms (e.g., Villalobos Herrera et al. 2023), while the coefficient of variation is a standard feature in stochastic analysis that can also be used to quantify gradients of variability. To maintain simplicity and avoid redundancy, we did not employ more features for the clustering.

To address scalability challenges (specifically, the large RAM storage requirements) posed by our large dataset (Section 4.1), which could not be handled by conventional non-hierarchical clustering algorithms (e.g., the well-known k-means and k-medoids described in detail in Hastie et al. 2009, ch. 14.3.6 and 14.3.10), we selected CLARA

(Clustering Large Applications; Kaufman and Rousseeuw 1990, ch. 3) as the core algorithm. In summary, CLARA is a resampling-based partitioning algorithm (Hopke and Kaufman 1990) applying k-medoids. These exhibit larger robustness to noise and outliers with respect to k-means, as they use actual data points (the "medoids") as cluster centers instead of computing their cluster centers (the "centroids"). Within CLARA's framework, the k-medoids are applied to cluster a random sample of the data, with this process being repeated multiple times. The best clustering solution is then selected based on a minimum dissimilarity distance measure and finally applied to the entire dataset. In this study, the sample number and sample size were set to 10,000 and 1,000, respectively. The dissimilarities were calculated using Euclidean distances.

To ensure that CLARA would not be affected by skewness and different scales in the features, feature preprocessing took place. More precisely, the feature values were first transformed and then standardized. Log-transformation was applied to the maximum intensity, total volume and total duration, and square-root transformation was applied to the coefficient of variation (due to the existence of zeros in the values of this latter feature). Standardization of the storm duration and coefficient of variation took place for all the stations together, while it was done for each station separately, for the maximum intensity and total volume. This distinction was made because the latter two features are expected to strongly depend on local climatological conditions, in contrast to the former two (e.g., Avanzi et al. 2015).

4.4 Storm-level characteristics of the classes

The storm classes, obtained through clustering, were initially explored with the four driving features (Section 4.3) and through visual inspection of the storm-type-labelled precipitation storm time series. We then investigated the classes based on three storm-level features that were not involved in the clustering, specifically the month at the storm initiation (seasonality), solar time at the first occurrence of the maximum intensity (diurnal cycle; note that the maximum intensity may appear more than once in storm time series, especially for sub-hourly temporal resolutions) and lightning count. The month at the storm initiation was extracted from the storm time series (Section 4.2). The solar time at the (first) occurrence of the maximum intensity was chosen over the local time to better reflect the sun's position in the sky and its influence on storm dynamics. It was estimated based on the respective UTC time (which was extracted from the storm time series;

Section 4.2) and the longitude at the location of the storm. Lightning count validation was performed on a reduced but still large sample, due to limitations in the availability of lightning data (Section 4.1).

4.5 Spatial organization of the classes and key events

To ensure that the classes, identified from local time series, are meaningful, it is important to verify their spatial consistency. We therefore computed the occurrence rate of each storm class in the neighborhood of each given class on the same day. More precisely, we examined each storm in each station, inspecting the occurrence of the storm class itself as well as the occurrences of the remaining storm classes in distance intervals of: (0, 10], (10, 20], (20, 50], (50, 100], (100, 200], and (200, 500] km. We only included storms in this computation, meaning that dry stations in the neighborhood were not considered.

Additionally, we examined the spatial pattern of storm states across the Alpine range for eight case studies. These included three random dates in winter and early spring, as well as five dates when events that are well-known to the research community occurred in the region, including the Vaia storm (Davolio et al. 2020), the Lausanne flood (Gabella et al. 2019), the Vizze flood (Destro et al. 2018), the Magra flood (Amponsah et al. 2016), and the Lierza flood (Borga et al. 2019). These selected benchmark events have been comprehensively documented and characterized in the literature as either "convective" or "stratiform" drawing on radar investigations, thereby providing a reliable reference for capturing possible linkages to precipitation processes.

4.6 Storm type climatology analysis

We performed a climatology analysis of the storm classes based on three independent parts. In the first, we computed the aggregate occurrence rates of each class at each geographical location (all years and seasons combined). In the second part, we computed seasonal (DJF, MAM, JJA, SON) occurrences within each class at each geographical location. To make the identification of spatial patterns easier, the occurrence rates (%) were grouped into 10% intervals, ranging from [0, 10] to (90, 100]. Then, we analyzed the climatological variations in time, following two steps: (a) computation of the occurrence rates of the classes within each of the consecutive time periods 1981-1990, 1991-2000, 2001-2010, and 2011-2023; and (b) trend analysis for 113 stations with at least 30 complete years of precipitation data (Figure S1). The latter comprised the computation of the slope of the linear regression line and performance of the Man-Kendall trend test

(Mann 1945; Kendall 1975), with the null hypothesis being correlation zero (no monotonic trend) and p-values smaller or equal to 0.05 suggesting strong evidence against the null hypothesis and, thus, trend. Both (a) and (b) were conducted for three different settings: all seasons combined; summer only (JJA); and the remaining seasons (DJF, MAM and SON).

Acknowledgements: This study was carried out within the RETURN Extended Partnership, funded by the European Union Next-GenerationEU (National Recovery and Resilience Plan – NRRP, Mission 4, Component 2, Investment 1.3 – D.D. 1243 2/8/2022, PE0000005), and within the Space It Up project, funded by the Italian Space Agency, ASI and the Ministry of University and Research, MUR, under contract n. 2024-5-E.0 - CUP n. I53D24000060005. FM was supported by the "The Geosciences for Sustainable Development" project (Budget Ministero dell'Università e della Ricerca–Dipartimenti di Eccellenza 2023–2027 C93C23002690001). ED was supported by "Programma Fondo Europeo di Sviluppo Regionale (FESR) 2021-2027 della Provincia autonoma di Trento", CUP C65E25000120001. MA was supported by the Med World consortium, funded by the Council for Higher Education in Israel; and by the Israel Science Foundation research grant (ISF's No. 4089/25) and the Maimonides Fund's Future Scientists Center. We thank Marika Koukoula and Nadav Peleg for handling parts of the rain gauge data. We also gratefully acknowledge the WWLLN consortium for generously providing the lightning data.

Appendix A Open science and data availability

Statistical software for reproducing the analysis is reported in Text S4 (Supplement). Information on the 792,786 precipitation storm time series extracted and analyzed in this study is provided as an open dataset (Papacharalampous et al. 2026). This dataset includes the precipitation storm series, without timestamps or coordinates but labelled by storm type (as "type-1 major", "type-2 major", "moderate", "type-1 minor", or "type-2 minor"). A separate set of information provides the geographical location where each storm was observed indicated by its longitude and latitude, the timestamps at the storm initiation and termination, the storm features that drove the proposed typology on an algorithmic basis (i.e., maximum intensity, total volume, total duration, and coefficient of variation), and the storm type. The two sets of information use different storm identifiers; thus, they are not linkable. The labelled storm series can support, for example, analysis of

storm-level characteristics of Alpine storms, validation of the typology using alternative clustering methods, or synthetic storm generation. The remaining information can support, for instance, spatially and temporally explicit analyses of Alpine storm characteristics, their drivers when combined with external time series or other additional data, and further validation of the typology using other datasets or independent event catalogues. The original time series cannot be shared by the authors. Their sources are:

- Agenzia Regionale per la Prevenzione e Protezione Ambientale del Veneto (https://www.arpa.veneto.it).
- Autorità di Bacino Distrettuale Fiume Po (https://www.adbpo.it).
- GeoSphere Austria (https://data.hub.geosphere.at/dataset/klima-v1-10min).
- Météo-France (https://meteo.data.gouv.fr).
- MeteoSwiss (https://www.meteoswiss.admin.ch).
- Provincia Autonoma di Bolzano (https://meteo.provincia.bz.it/default.asp).
- Provincia Autonoma di Trento (https://www.provincia.tn.it).

References

Amponsah W, Marchi L, Zoccatelli D, Boni G, Cavalli M, Comiti F, Crema S, Lucía A, Marra F, Borga M (2016) Hydrometeorological characterisation of a flash flood associated with major geomorphic effects: Assessment of peak discharge uncertainties and analysis of the runoff response, Journal of Hydrometeorology 17:3063–3077. https://doi.org/10.1175/JHM-D-16-0081.1.

Araujo DS, Marra F, Ali H, Fowler HJ, Nikolopoulos EI (2023) Relation between storm characteristics and extreme precipitation statistics over CONUS. Advances in Water Resources 178:104497. https://doi.org/10.1016/j.advwatres.2023.104497.

Avanzi F, De Michele C, Gabriele S, Ghezzi A, Rosso R (2015) Orographic signature on extreme precipitation of short durations. Journal of Hydrometeorology 16:278–294. https://doi.org/10.1175/JHM-D-14-0063.1.

Beck HE, McVicar TR, Vergopolan N, Berg A, Lutsko NJ, Dufour A, Zeng Z, Jiang X, Van Dijk AI, Miralles DG (2023) High-resolution (1 km) Köppen-Geiger maps for 1901–2099 based on constrained CMIP6 projections. Scientific Data 10(1):724. https://doi.org/10.1038/s41597-023-02549-6.

Blanchet J, Reverdy A, Blanc A, Creutin JD, Kiennemann P, Evin G (2025) Linking torrential flood event occurrence to weather-type conditional driving atmospheric conditions—The case of the Northern French Alps. Journal of Hydrology: Regional Studies 59:102402. https://doi.org/10.1016/j.ejrh.2025.102402.

Blöschl G, Bierkens MFP, Chambel A, Cudennec C, Destouni G, Fiori A, Kirchner JW, McDonnell JJ, Savenije HHG, Sivapalan M, et al. (2019) Twenty-three Unsolved Problems in Hydrology (UPH) – A community perspective. Hydrological Sciences Journal 64(1):1141–1158. https://doi.org/10.1080/02626667.2019.1620507.

Borga M, Comiti F, Ruin I, Marra F (2019) Forensic analysis of flash flood response. Wiley Interdisciplinary Reviews: Water 6(2):e1338. https://doi.org/10.1002/wat2.1338.

Borga M, Vezzani C, Dalla Fontana G (2005) Regional rainfall depth–duration–frequency equations for an alpine region. Natural Hazards 36(1):221–235. https://doi.org/10.1007/s11069-004-4550-y.

Breugem AJ, Wesseling JG, Oostindie K, Ritsema CJ (2020) Meteorological aspects of heavy precipitation in relation to floods–an overview. Earth-Science Reviews 204:103171. https://doi.org/10.1016/j.earscirev.2020.103171.

Buzzi A, Tartaglione N, Malguzzi P (1998) Numerical simulations of the 1994 Piedmont flood: Role of orography and moist processes. Monthly Weather Review 126(9):2369–2383. https://doi.org/10.1175/1520-0493(1998)126<2369:NSOTPF>2.0.CO;2.

Cipolla G, Francipane A, Noto L (2020) Classification of extreme rainfall for a Mediterranean region by means of atmospheric circulation patterns and reanalysis data. Water Resources Management 34(10):3219–3235. https://doi.org/10.1007/s11269-020-02609-1.

Correa-Sánchez N, Dallan E, Marra F, Fosser G, Borga M (2025) Orographic control on bias and uncertainty in extreme sub-daily precipitation simulations from a convection-permitting ensemble. Journal of Hydrology 659:133324. https://doi.org/10.1016/j.jhydrol.2025.133324.

Dallan E, Borga M, Zaramella M, Marra F (2022) Enhanced summer convection explains observed trends in extreme subdaily precipitation in the Eastern Italian Alps. Geophysical Research Letters 49(5):e2021GL096727. https://doi.org/10.1029/2021GL096727.

Dallan E, Marra F, Fosser G, Marani M, Formetta G, Schär C, Borga M (2023) How well does a convection-permitting regional climate model represent the reverse orographic effect of extreme hourly precipitation?. Hydrology and Earth System Sciences 27(5):1133–1149. https://doi.org/10.5194/hess-27-1133-2023.

Dallan E, Borga M, Fosser G, Canale A, Roghani B, Marani M, Marra F (2024) A method to assess and explain changes in sub-daily precipitation return levels from convection-permitting simulations. Water Resources Research 60(5):e2023WR035969. https://doi.org/10.1029/2023WR035969.

Dallan E, Marra F, Papacharalampous GA, Fowler H, Borga M (2025) Climatology of storm characteristics for sub-daily heavy precipitation in the Greater Alpine Region. ESS Open Archive. https://doi.org/10.22541/essoar.176487365.52815673/v1.

Davolio S, Della Fera S, Laviola S, Miglietta MM, Levizzani V (2020) Heavy precipitation over Italy from the Mediterranean storm "Vaia" in October 2018: Assessing the role of an atmospheric river. Monthly Weather Review 148(9):3571–3588. https://doi.org/10.1175/MWR-D-20-0021.1.

Destro E, Amponsah W, Nikolopoulos EI, Marchi L, Marra F, Zoccatelli D, Borga M (2018) Coupled prediction of flash flood response and debris flow occurrence: Application on an alpine extreme flood event. Journal of Hydrology 558:225–237. https://doi.org/10.1016/j.jhydrol.2018.01.021.

D'Odorico P, Fagherazzi S, Rigon R (2005) Potential for landsliding: Dependence on hyetograph characteristics. Journal of Geophysical Research: Earth Surface 110(F1). https://doi.org/10.1029/2004JF000127.

Estermann R, Rajczak J, Velasquez P, Lorenz R, Schär C (2025) Projections of heavy precipitation characteristics over the greater Alpine region using a kilometer–scale climate model ensemble. Journal of Geophysical Research: Atmospheres 130(2):e2024JD040901. https://doi.org/10.1029/2024JD040901.

Feloni EG, Baltas EA, Nastos PT, Matsangouras IT (2019) Implementation and evaluation of a convective/stratiform precipitation scheme in Attica region, Greece. Atmospheric Research 220:109–119. https://doi.org/10.1016/j.atmosres.2019.01.011.

Fischer S, Schumann AH (2024) Temporal changes in the frequency of flood types and their impact on flood statistics. Journal of Hydrology X 22:100171. https://doi.org/10.1016/j.hydroa.2024.100171.

Fischer S, Schumann AH (2021) Regionalisation of flood frequencies based on flood type-specific mixture distributions. Journal of Hydrology X 13:100107. https://doi.org/10.1016/j.hydroa.2021.100107.

Fischer S, Schumann A, Bühler P (2019) Timescale-based flood typing to estimate temporal changes in flood frequencies. Hydrological Sciences Journal 64(15):1867–1892. https://doi.org/10.1080/02626667.2019.1679376.

Flaounas E, Aragão L, Bernini L, Dafis S, Doiteau B, Flocas H, Gray SL, Karwat A, Kouroutzoglou J, Lionello P, et al. (2023) A composite approach to produce reference datasets for extratropical cyclone tracks: Application to Mediterranean cyclones, Weather and Climate Dynamics 4:639–661. https://doi.org/10.5194/wcd-4-639-2023.

Frei C, Schär C (1998) A precipitation climatology of the Alps from high-resolution rain-gauge observations. International Journal of Climatology: A Journal of the Royal Meteorological Society 18(8):873–900. https://doi.org/10.1002/(SICI)1097-0088(19980630)18:8%3C873::AID-JOC255%3E3.0.CO;2-9.

Grazzini F, Craig GC, Keil C, Antolini G, Pavan V (2020) Extreme precipitation events over northern Italy. Part I: A systematic classification with machine-learning techniques. Quarterly Journal of the Royal Meteorological Society 146(726):69–85. https://doi.org/10.1002/qj.3635.

Gustafsson N, Janjić T, Schraff C, Leuenberger D, Weissmann M, Reich H, Brousseau P, Montmerle T, Wattrelot E, Bučánek A, et al. (2018) Survey of data assimilation methods for convective-scale numerical weather prediction at operational centres. Quarterly Journal of the Royal Meteorological Society 144(713): 1218–1256. https://doi.org/10.1002/qj.3179.

Hastie T, Tibshirani R, Friedman J (2009) The Elements of Statistical Learning: Data Mining, Inference and Prediction, second edition. Springer, New York. https://doi.org/10.1007/978-0-387-84858-7.

Hirschboeck KK (1988) Flood Hydroclimatology. In: Baker VR, Kochel RC, Patton PC (Eds) Flood Geomorphology. Wiley-Interscience.

Hopke PK, Kaufman L (1990) The use of sampling to cluster large data sets. Chemometrics and Intelligent Laboratory Systems 8(2):195–204. https://doi.org/10.1016/0169-7439(90)80135-S.

Isotta FA, Frei C, Weilguni V, Percec Tadic M, Lassegues P, Rudolf B, Pavan V, Cacciamani C, Antolini G, Ratto SM, et al. (2014) The climate of daily precipitation in the Alps: Development and analysis of a high-resolution grid dataset from pan-Alpine rain-gauge data. International Journal of Climatology 34(5):1657–1675. https://doi.org/10.1002/joc.3794.

James G, Witten D, Hastie T, Tibshirani R (2013) An Introduction to Statistical Learning. Springer, New York. https://doi.org/10.1007/978-1-4614-7138-7.

Kaczmarska J, Isham V, Onof C (2014) Point process models for fine-resolution rainfall. Hydrological Sciences Journal 59(11):1972–1991. https://doi.org/10.1080/02626667.2014.925558.

Kahraman A, Kendon EJ, Chan SC, Fowler HJ (2021) Quasi-stationary intense rainstorms spread across Europe under climate change. Geophysical Research Letters 48(13):e2020GL092361. https://doi.org/10.1029/2020GL092361.

Kahraman A, Kendon EJ, Fowler HJ, Wilkinson JM (2022) Contrasting future lightning stories across Europe. Environmental Research Letters 17(11):114023. https://doi.org/10.1088/1748-9326/ac9b78.

Kaufman L, Rousseeuw PJ (1990) Finding Groups in Data: An Introduction to Cluster Analysis. Wiley, New York.

Kendall MG (1975) Rank Correlation Methods, fourth edition. Charles Griffin, London.

Laaha G, Laimighofer J, Özcelik NB, Fischer S (2025) Exploring process heterogeneity in environmental statistics: Examples and methodological advances. Austrian Journal of Statistics 54(3):124–149. https://doi.org/10.17713/ajs.v54i3.2101.

Llasat MC, del Moral A, Cortès M, Rigo T (2021) Convective precipitation trends in the Spanish Mediterranean region. Atmospheric Research 257:105581. https://doi.org/10.1016/j.atmosres.2021.105581.

Mann HB (1945) Non-parametric tests against trend. Econometrica 13:163–171. https://doi.org/10.2307/1907187.

Maraun D, Shepherd TG, Widmann M, Zappa G, Walton D, Gutiérrez JM, Hagemann S, Richter I, Soares PMM, Hall A, Mearns LO (2017) Towards process-informed bias correction of climate change simulations. Nature Climate Change 7(11):764–773. https://doi.org/10.1038/nclimate3418.

Markonis Y, Kumar R, Hanel M, Rakovec O, Máca P, AghaKouchak A (2021) The rise of compound warm-season droughts in Europe. Science Advances 7(6):eabb9668. https://doi.org/10.1126/sciadv.abb9668.

Marra F, Nikolopoulos EI, Creutin JD, Borga M (2014) Radar rainfall estimation for the identification of debris-flow occurrence thresholds. Journal of Hydrology 519(Part B):1607–1619. https://doi.org/10.1016/j.jhydrol.2014.09.039.

Marra F, Borga M, Morin E (2020) A unified framework for extreme subdaily precipitation frequency analyses based on ordinary events. Geophysical Research Letters 47(18):e2020GL090209. https://doi.org/10.1029/2020GL090209.

Marra F, Armon M, Adam O, Zoccatelli D, Gazal O, Garfinkel CI, Rostkier-Edelstein D, Dayan U, Enzel Y, Morin E (2021) Toward narrowing uncertainty in future projections of local extreme precipitation. Geophysical Research Letters 48(5):e2020GL091823. https://doi.org/10.1029/2020GL091823.

Marra F, Koukoula M, Canale A, Peleg N (2024) Predicting extreme sub-hourly precipitation intensification based on temperature shifts. Hydrology and Earth System Sciences 28(2):375–389. https://doi.org/10.5194/hess-28-375-2024.

Marra F, Dallan E, Canale A, Prosdocimi I, Papacharalampous GA, Borga M, Papalexiou SM (2026) Apparent heavy tails of sub-daily precipitation explained by the coexistence of lighter-tailed processes. Geophysical Research Letters 53(2):e2025GL119705. https://doi.org/10.1029/2025GL119705.

Ménégoz M, Valla E, Jourdain NC, Blanchet J, Beaumet J, Wilhelm B, Gallée H, Fettweis X, Morin S, Anquetin S (2020) Contrasting seasonal changes in total and intense precipitation in the European Alps from 1903 to 2010. Hydrology and Earth System Sciences 24(11):5355–5377. https://doi.org/10.5194/hess-24-5355-2020.

Merz B, Aerts J, Arnbjerg-Nielsen K, Baldi M, Becker A, Bichet A, Blöschl G, Bouwer LM, Brauer A, Cioffi F, et al. (2014) Floods and climate: Emerging perspectives for flood risk assessment and management. Natural Hazards and Earth System Sciences 14:1921–1942. https://doi.org/10.5194/nhess-14-1921-2014.

Merz R, Blöschl G (2003) A process typology of regional floods. Water Resources Research 39(12). https://doi.org/10.1029/2002WR001952.
Napoli A, Parodi A, von Hardenberg J, Pasquero C (2023) Altitudinal dependence of projected changes in occurrence of extreme events in the Great Alpine Region. International Journal of Climatology 43(12):5813–5829. https://doi.org/10.1002/joc.8222.
Oppel H, Fischer S (2020) A new unsupervised learning method to assess clusters of temporal distribution of rainfall and their coherence with flood types. Water Resources Research 56(5):e2019WR026511. https://doi.org/10.1029/2019WR026511.
Papacharalampous GA, Dallan E, Armon M, Saha J, Price C, Borga M, Marra F (2026) Precipitation-driven typology of storms in the Alps: Data (Version v2) [Dataset]. Zenodo. https://doi.org/10.5281/zenodo.19264262.
Papadopoulos A, Chronis TG, Anagnostou EN (2005) Improving convective precipitation forecasting through assimilation of regional lightning measurements in a mesoscale model. Monthly Weather Review 133(7):1961–1977. https://doi.org/10.1175/MWR2957.1.
Peleg N, Morin E (2014) Stochastic convective rain-field simulation using a high-resolution synoptically conditioned weather generator (HiReS-WG). Water Resources Research 50(3):2124–2139. https://doi.org/10.1002/2013WR014836.
Peleg N, Koukoula M, Marra F (2025) A 2C warming can double the frequency of extreme summer downpours in the Alps. npj Climate and Atmospheric Science 8:216. https://doi.org/10.1038/s41612-025-01081-1.
Pineda N, Tomeu R, Joan B, Xavier S (2007) Lightning and precipitation relationship in summer thunderstorms: Case studies in the North Western Mediterranean region. Atmospheric Research 85(2):159–170. https://doi.org/10.1016/j.atmosres.2006.12.004.
Rodger CJ, Werner S, Brundell JB, Lay EH, Thomson NR, Holzworth RH, Dowden RL (2006) Detection efficiency of the VLF world-wide lightning location network (WWLLN): Initial case study. Annales Geophysicae 24(12):3197–3214. https://doi.org/10.5194/angeo-24-3197-2006.
Rubel F, Brugger K, Haslinger K, Auer I (2017) The climate of the European Alps: Shift of very high resolution Köppen-Geiger climate zones 1800–2100. Meteorologische Zeitschrift 26(2):115-125. https://doi.org/10.1127/metz/2016/0816.
Ruiz-Leo AM, Hernández E, Queralt S, Maqueda G (2013) Convective and stratiform precipitation trends in the Spanish Mediterranean coast. Atmospheric Research 119:46–55. https://doi.org/10.1016/j.atmosres.2011.07.019.
Rulfová Z, Kyselý J (2013) Disaggregating convective and stratiform precipitation from station weather data. Atmospheric Research 134:100–115. https://doi.org/10.1016/j.atmosres.2013.07.015.
Rulfová Z, Kyselý J (2014) Trends of convective and stratiform precipitation in the Czech Republic, 1982–2010. Advances in Meteorology 2014:647938. https://doi.org/10.1155/2014/647938.
Soriano LR, De Pablo F, Díez EG (2001) Relationship between convective precipitation and cloud-to-ground lightning in the Iberian Peninsula. Monthly Weather Review 129(12):2998–3003. https://doi.org/10.1175/1520-0493(2001)129<2998:RBCPAC>2.0.CO;2.

Sottile G, Francipane A, Adelfio G, Noto LV (2022) A PCA-based clustering algorithm for the identification of stratiform and convective precipitation at the event scale: An application to the sub-hourly precipitation of Sicily, Italy. Stochastic Environmental Research and Risk Assessment 36(8):2303–2317. https://doi.org/10.1007/s00477-021-02028-7.

Stein L, Pianosi F, Woods R (2020) Event-based classification for global study of river flood generating processes. Hydrological Processes 34(7):1514–1529. https://doi.org/10.1002/hyp.13678.

Tarasova L, Merz R, Kiss A, Basso S, Blöschl G, Merz B, Viglione A, Plötner S, Guse B, Schumann A, et al. (2019) Causative classification of river flood events. Wiley Interdisciplinary Reviews: Water 6(4):e1353. https://doi.org/10.1002/wat2.1353.

Tarasova L, Basso S, Wendi D, Viglione A, Kumar R, Merz R (2020) A process-based framework to characterize and classify runoff events: The event typology of Germany. Water Resources Research 56(5):e2019WR026951. https://doi.org/10.1029/2019WR026951.

Tremblay A (2005) The stratiform and convective components of surface precipitation. Journal of the Atmospheric Sciences 62(5):1513–1528. https://doi.org/10.1175/JAS3411.1.

Treppiedi D, Cipolla G, Noto LV (2023) Convective precipitation over a Mediterranean area: From identification to trend analysis starting from high-resolution rain gauges data. International Journal of Climatology 43(1):293–313. https://doi.org/10.1002/joc.7758.

Tseng CY, Wang LP, Onof C (2025) Modelling convective cell life cycles with a copula-based approach. Hydrology and Earth System Sciences 29(1):1–25. https://doi.org/10.5194/hess-29-1-2025.

Turkington T, Breinl K, Ettema J, Alkema D, Jetten V (2016) A new flood type classification method for use in climate change impact studies. Weather and Climate Extremes 14:1–16. https://doi.org/10.1016/j.wace.2016.10.001.

Villalobos Herrera R, Blenkinsop S, Guerreiro SB, Fowler HJ (2023) The creation and climatology of a large independent rainfall event database for Great Britain. International Journal of Climatology 43(13):6020–6037. https://doi.org/10.1002/joc.8187.

Virts KS, Wallace JM, Hutchins ML, Holzworth RH (2013) Highlights of a new ground-based, hourly global lightning climatology. Bulletin of the American Meteorological Society 94(9):1381–1391. https://doi.org/10.1175/bams-d-12-00082.1.

Weisse AK, Bois P (2001) Topographic effects on statistical characteristics of heavy rainfall and mapping in the French Alps. Journal of Applied Meteorology 40(4):720–740. https://doi.org/10.1175/1520-0450(2001)040<0720:TEOSCO>2.0.CO;2.

Zhou K, Zheng Y, Li B, Dong W, Zhang X (2019) Forecasting different types of convective weather: A deep learning approach. Journal of Meteorological Research 33:797–809. https://doi.org/10.1007/s13351-019-8162-6.

Supplement

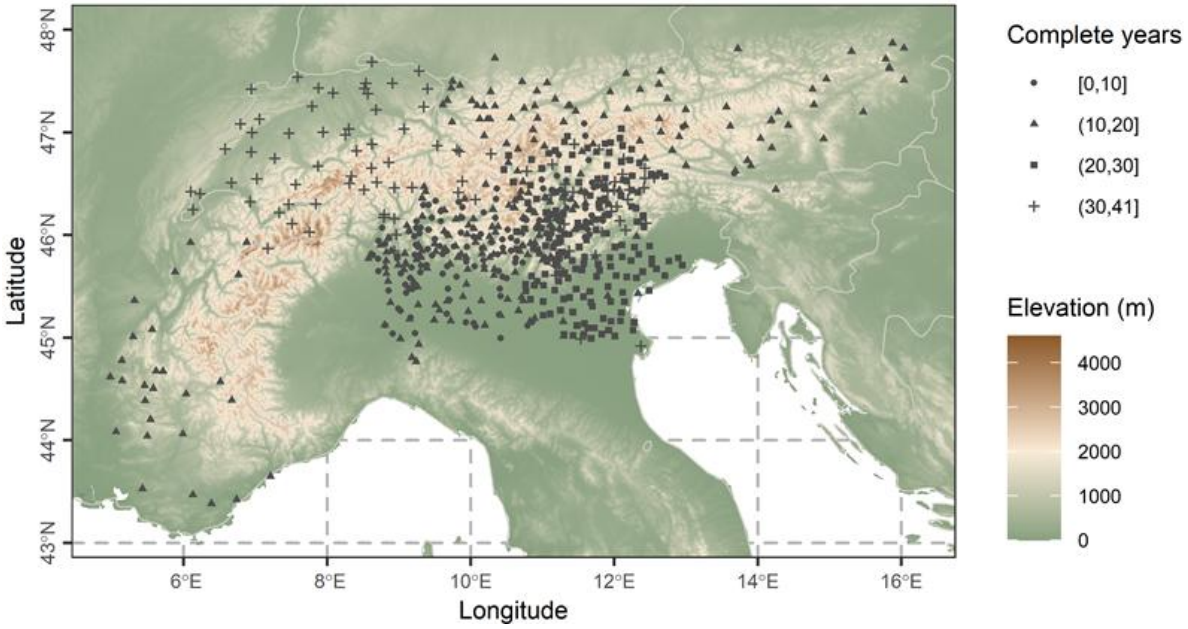

Figure S1. Study area, its topography (extracted from the Amazon Web Services Terrain Tiles), geographical locations of the precipitation stations and number of complete years of available data for each of these stations.

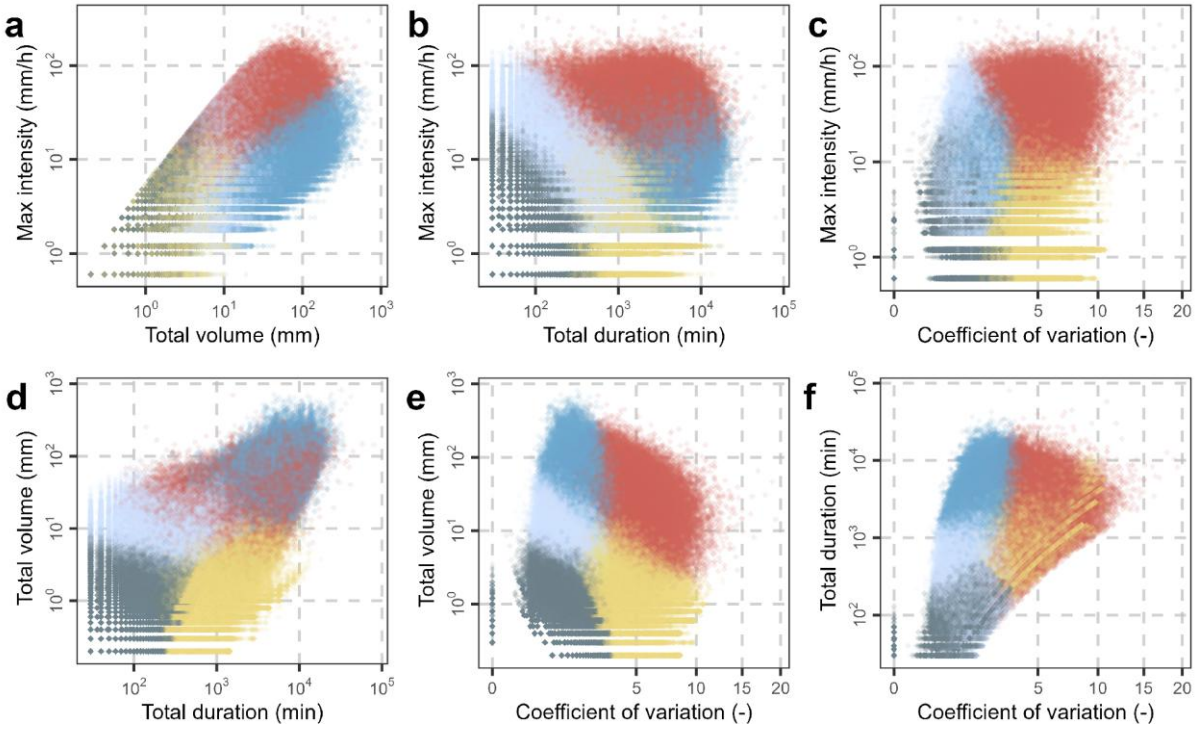

Figure S2. Investigations of the relationships between the maximum intensity, total volume, total duration and coefficient of variation values characterizing the clusters.

Text S1. Spatial organization of the classes.

Spatial organization characterizes the historical occurrences of all storm classes, with each of them having occurred far more frequently in the vicinity of its own events on the same day than any other class, at least for distances up to 50 km (Figure S3; see the side-by-side boxplots on the main diagonal thereon). The "type-2 major" class exhibits the largest degree of spatial clustering. Its historical occurrence rates exhibit a median equal to about 75% for distances smaller than 10 km, meaning that storms observed within 10 km from a "type-2 major" storm are classified as the same type about 75% of the time. This median gradually decreases to about 50% for distances of 200 to 500 km from the analyzed storm. The "type-1 major" class exhibits the second largest degree of spatial clustering, with median occurrence rates around 65% at distances smaller than 10 km, decreasing to still more than 30% at 200–500 km distances. With the respective occurrence rates being found equal to about 55% and larger than 15%, the "moderate" class exhibits the third largest degree of spatial clustering and graduality in the reduction of these rates with the distance. From a different angle, the distances at which the median rates are closest to 50% are 100, 200 and 20 km for the "type-1 major", "type-2 major" and "moderate" classes, respectively.

For the "type-1 minor" and "type-2 minor" classes, the reduction in the occurrence rates with distance is more abrupt. This aligns with our expectations, as these classes are anticipated to correspond to unimportant storms or phenomena that were not well-captured by our gauges. For example, we expect the stations that only capture the outermost portions of an important event to only see a minor amount of precipitation. Indeed, the median of these rates starts from about 40% for distances less than 10 km and becomes less than 25% already for distances between 20 and 50 km. Moreover, as the distance from a storm observation increases, the occurrence rates of different classes increase notably for some pairs of classes, such as the {"type-2 major", "type-1 major"} and {"type-2 major", "moderate"}. For other pairs, they remain similar or tend to only slightly increase.

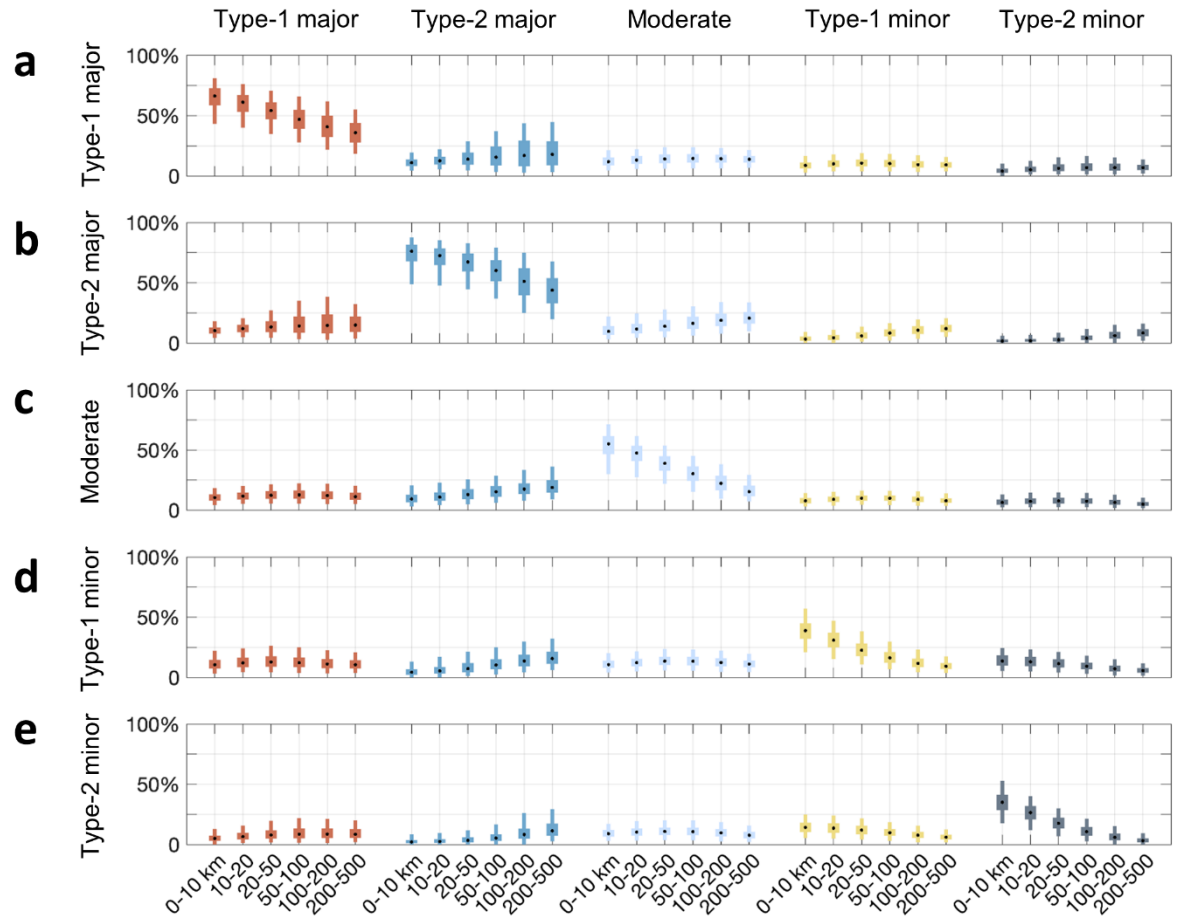

Figure S3. Occurrence rates of the classes in the wet stations within various ranges of distances from the (a) “type-1 major”, (b) “type-2 major”, (c) "moderate", (d) “type-1 minor” and (e) “type-2 minor” classes.

Text S2. Historical proportions of the storm class occurrences across the Alpine range.

Figure S4 illustrates the historical proportions of the classes across the examined locations. Overall, “type-1 major” storms (Figure S4a) occurred at rates between 10% and 20% in many locations, including those in Switzerland and Germany, most of those in France and Austria, and about half of those in Italy. In the remaining locations, mostly including the largest part of Northeastern Italy, “type-1 major” storm occurrence ranged from 20% and 30%. The “type-2 major” storms (Figure S4b) were prevalent, occurring at rates from 20% to 30% in most Italian areas and some locations in France, Switzerland, Germany, and Austria. Higher occurrences, between 30% and 40%, were observed at almost all the remaining locations. Only a few lowland locations in Italy showed lower occurrences of this storm type. Rates of the “moderate” storms (Figure S4c) were more consistent across the various locations, with most experiencing occurrences between 20% and 30%. Small variations existed, with a few locations exhibiting rates slightly outside this range. Lastly, each of the minor classes (Figure S4d, e) generally represented 10% to 20% of the occurrences for most locations. However, the “type-1 minor” storms (Figure S4d) were more frequent (largely 20%-30%) for most of the examined lowland locations in Italy.

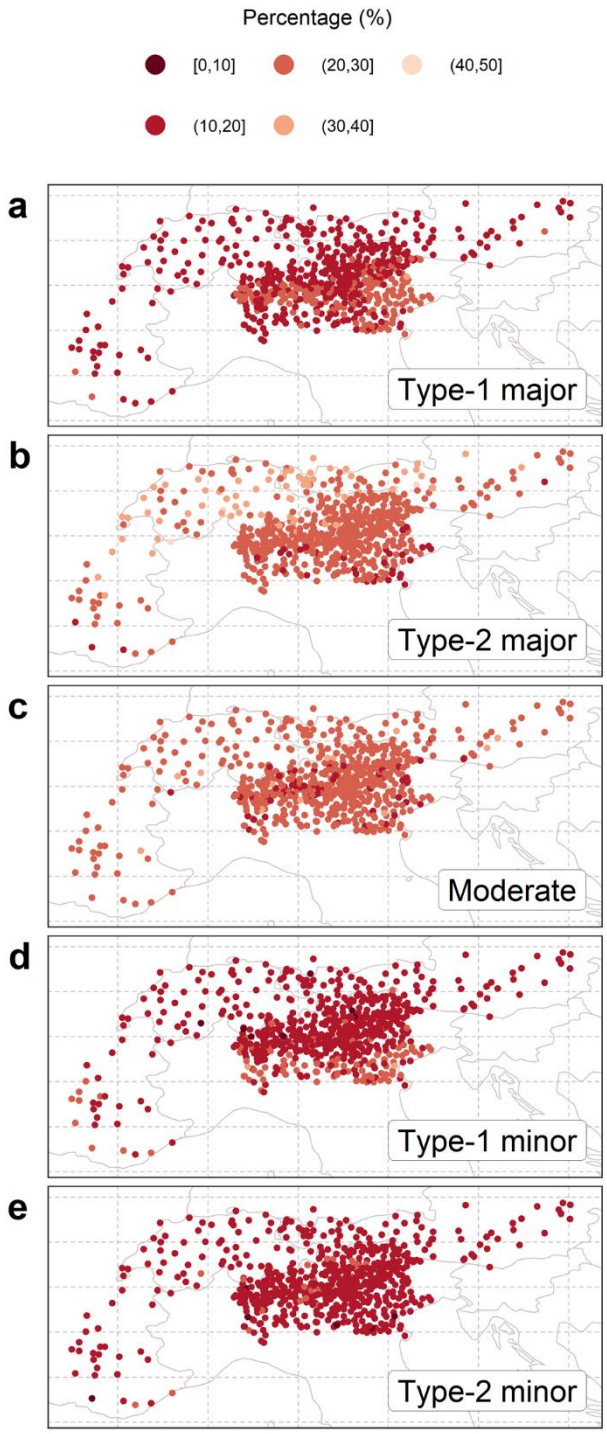

Figure S4. Proportions of the (a) “type-1 major”, (b) “type-2 major”, (c) “moderate”, (d) ”type-1 minor” and (e) “type-2 minor” classes in each geographical location.

Text S3. Seasonal occurrence rates of the classes across the Alpine range.

Distinct spatial patterns were identified in the seasonal occurrence rates of the "type-1 major" (Figure S5a, d, g, j) and "type-2 major" (Figure S5b, e, h, k) storm classes across the four seasons. For nearly all locations, the "type-1 major" class occurred at very low rates during winter (DJF), as also shown in Figure S5e, resulting in no notable spatial patterns for that season (Figure S5a). In contrast, "type-1 major" storms are most frequent in summer (JJA), and their occurrence rates (Figure S5g) reveal clear meteorological differences across regions, with rates increasing from south (40–50% at most locations) to north (50–80%) and from lowlands to highlands. In the spring (MAM) and autumn (SON), "type-1 major" storms appeared more often in low-elevation locations in Italy (rates 20–30% at most of them) than in the pre-Alps and Alps (rates below 20% at most locations). In the same seasons, the "type-2 major" storms showed high occurrence rates (40–50% at most locations), which however do not reveal clear spatial patterns. In the winter, they mostly occurred with lower rates for the pre-Alpine and Alpine areas in Italy (below 30%) than for other regions, while in the summer they occurred with low rates (below 10%) for the low-elevation locations in Italy and for southern locations in France and with somewhat larger rates (mostly 10–30%) for the remaining regions, likely reflecting a south-north gradient. Meanwhile, no notable spatial patterns were observed for the "moderate" storms across the four seasons (Figure S5c, f, i, l).

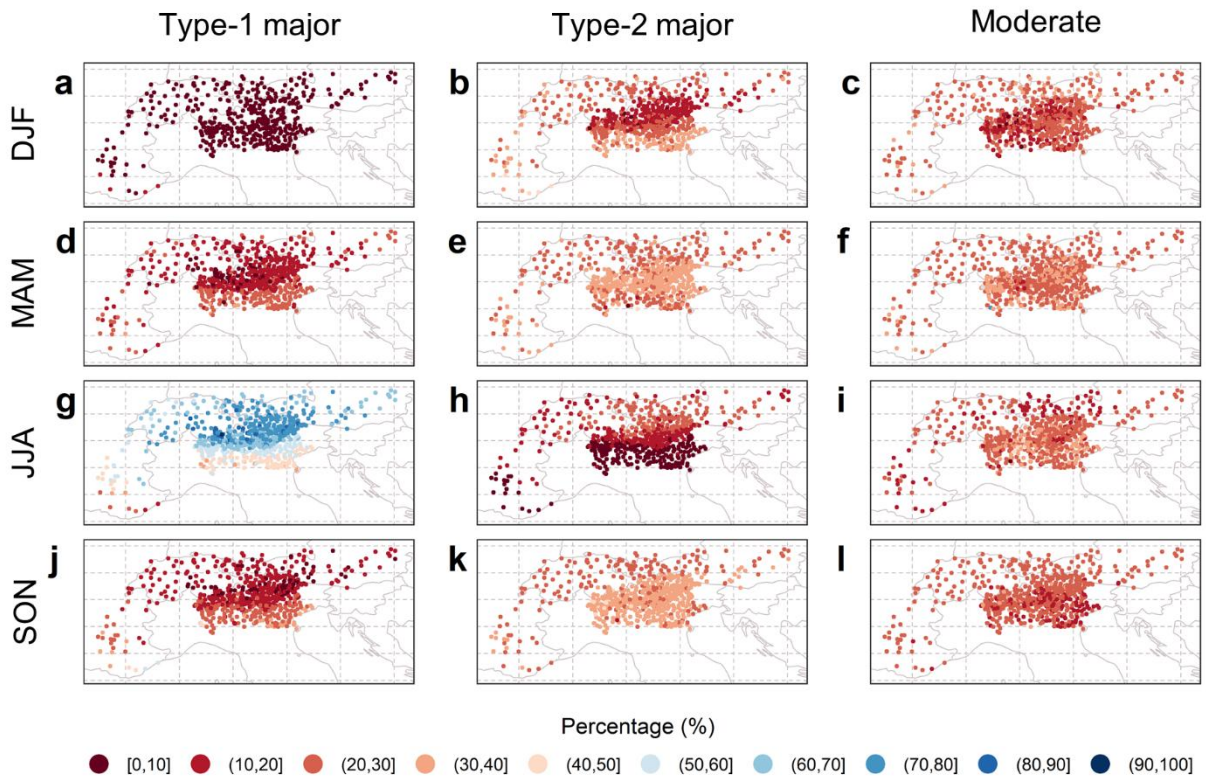

Figure S5. Proportions of the seasons within the (a, d, g, j) "type-1 major", (b, e, h, k) "type-2 major" and (c, f, i, l) "moderate" classes.

Text S4. Statistical software information.

Data processing relied on a combination of `R` (R Core Team 2024) and `MATLAB`. Statistical analyses and visualizations were conducted in `R`, aside from part of the computational analyses on spatial clustering, including the creation of Figure S3, which were performed in `MATLAB`. The following `R` packages were utilized: `bdc` (Ribeiro et al. 2024), `cluster` (Maechler et al. 2023), `data.table` (Barrett et al. 2024), `devtools` (Wickham et al. 2022), `dplyr` (Wickham et al. 2023a), `elevatr` (Hollister 2023), `ggpubr` (Kassambara 2023), `ggridges` (Wilke 2024), `gplots` (Warnes et al. 2024), `knitr` (Xie 2014, 2015, 2024), `lubridate` (Grolemund and Wickham 2011, Spinu et al. 2024), `raster` (Hijmans 2025), `RColorBrewer` (Neuwirth 2022), `readxl` (Wickham and Bryan 2023), `rmarkdown` (Allaire et al. 2024, Xie et al. 2018, 2020), `rnaturalearth` (Massicotte and South 2023), `scales` (Wickham et al. 2023b), `streamMetabolizer` (Appling et al. 2018) and `tidyverse` (Wickham et al. 2019, Wickham 2023). Equivalent codes to those used for extracting the precipitation storm time series in this study can be found in Marra (2024).

References

Allaire JJ, Xie Y, Dervieux C, McPherson J, Luraschi J, Ushey K, Atkins A, Wickham H, Cheng J, Chang W, Iannone R (2024) rmarkdown: Dynamic Documents for R. R package version 2.29. https://CRAN.R-project.org/package=rmarkdown.

Appling AP, Hall Jr RO, Yackulic CB, Arroita M (2018) Overcoming equifinality: Leveraging long time series for stream metabolism estimation. Journal of Geophysical Research: Biogeosciences 123(2):624–645. https://doi.org/10.1002/2017JG004140.

Barrett T, Dowle M, Srinivasan A, Gorecki J, Chirico M, Hocking T, Schwendinger B (2024) data.table: Extension of 'data.frame'. R package version 1.16.4. https://CRAN.R-project.org/package=data.table.

Grolemund G, Wickham H (2011) Dates and times made easy with lubridate. Journal of Statistical Software 40(3):1–25. https://doi.org/10.18637/jss.v040.i03.

Hijmans R (2025) raster: Geographic Data Analysis and Modeling. R package version 3.6-31. https://CRAN.R-project.org/package=raster.

Hollister JW (2023) elevatr: Access Elevation Data from Various APIs. R package version 0.99.0. https://CRAN.R-project.org/package=elevatr.

Kassambara A (2023) ggpubr: 'ggplot2' Based Publication Ready Plots. R package version 0.6.0. https://CRAN.R-project.org/package=ggpubr.

Maechler M, Rousseeuw P, Struyf A, Hubert M, Hornik K (2023) cluster: Cluster Analysis Basics and Extensions. R package version 2.1.6. https://CRAN.R-project.org/package=cluster.

Marra F (2024) A unified framework for extreme sub-daily precipitation frequency analyses based on ordinary events - data & codes. (Version v1.2) [Software]. Zenodo. https://doi.org/10.5281/zenodo.11934843.

Massicotte P, South A (2023) rnaturalearth: World Map Data from Natural Earth. R package version 1.0.1. https://CRAN.R-project.org/package=rnaturalearth.

Neuwirth E (2022) RColorBrewer: ColorBrewer Palettes. R package version 1.1-3. https://CRAN.R-project.org/package=RColorBrewer.

R Core Team (2024) R: A language and environment for statistical computing. R Foundation for Statistical Computing, Vienna, Austria. https://www.r-project.org.
Ribeiro B, Velazco S, Guidoni-Martins K, Tessarolo G, Jardim L (2024) bdc: Biodiversity Data Cleaning. R package version 1.1.5. https://CRAN.R-project.org/package=bdc.
Spinu V, Grolemund G, Wickham H (2024) lubridate: Make Dealing with Dates a Little Easier. R package version 1.9.4. https://CRAN.R-project.org/package=lubridate.
Warnes G, Bolker B, Bonebakker L, Gentleman R, Huber W, Liaw A, Lumley T, Maechler M, Magnusson A, Moeller S, et al. (2024) gplots: Various R Programming Tools for Plotting Data. R package version 3.2.0. https://CRAN.R-project.org/package=gplots.
Wickham H (2023) tidyverse: Easily Install and Load the 'Tidyverse'. R package version 2.0.0. https://CRAN.R-project.org/package=tidyverse.
Wickham H, Averick M, Bryan J, Chang W, McGowan LD, François R, Grolemund G, Hayes A, Henry L, Hester J, et al. (2019) Welcome to the tidyverse. Journal of Open Source Software 4(43):1686. https://doi.org/10.21105/joss.01686.
Wickham H, Bryan J (2023) readxl: Read Excel Files. R package version 1.4.3. https://CRAN.R-project.org/package=readxl.
Wickham H, Hester J, Chang W, Bryan J (2022) devtools: Tools to Make Developing R Packages Easier. R package version 2.4.5. https://CRAN.R-project.org/package=devtools.
Wickham H, François R, Henry L, Müller K, Vaughan D (2023a) dplyr: A Grammar of Data Manipulation. R package version 1.1.4. https://CRAN.R-project.org/package=dplyr.
Wickham H, Pedersen T, Seidel D (2023b) scales: Scale Functions for Visualization. R package version 1.3.0. https://CRAN.R-project.org/package=scales.
Wilke C (2024) ggridges: Ridgeline Plots in 'ggplot2'. R package version 0.5.6. https://CRAN.R-project.org/package=ggridges.
Xie Y (2014) knitr: A Comprehensive Tool for Reproducible Research in R. In: Stodden V, Leisch F, Peng RD (Eds) Implementing Reproducible Computational Research. Chapman and Hall/CRC.
Xie Y (2015) Dynamic Documents with R and knitr, second edition. Chapman and Hall/CRC.
Xie Y (2024) knitr: A General-Purpose Package for Dynamic Report Generation in R. R package version 1.49. https://CRAN.R-project.org/package=knitr.
Xie Y, Allaire JJ, Grolemund G (2018) R Markdown: The Definitive Guide. Chapman and Hall/CRC. ISBN 9781138359338. https://bookdown.org/yihui/rmarkdown.
Xie Y, Dervieux C, Riederer E (2020) R Markdown Cookbook. Chapman and Hall/CRC. ISBN 9780367563837. https://bookdown.org/yihui/rmarkdown-cookbook.